Pergamon

Cement and Concrete Research 33 (2003) 103–113

CEMENT AND CONCRETE RESEARCH

A multiscale model for effective moduli of concrete incorporating ITZ water–cement ratio gradients, aggregate size distributions, and entrapped voids

J.C. Nadeau*

Department of Civil and Environmental Engineering, Duke University, 121 Hudson Hall Box 90287, Durham, NC 27708-0287, USA

Received 4 January 2002; accepted 9 July 2002

Abstract

This paper develops a model for the effective elastic properties of concrete, which is a function of the volume fractions, size distributions, and elastic properties of fine aggregate (FA) and coarse aggregate (FA) and entrapped voids. Furthermore, the model is a function of the overall water–cement ratio and specific gravity of cement. Explicitly modeled are the water–cement ratio gradients through the interfacial transition zone (ITZ), which, in turn, affect the variation of the cement paste elastic properties through the ITZ, while maintaining the total fractions of cement and water consistent with the overall water–cement ratio. The ITZ volume is also conserved.

Keywords: Interfacial transition zone; Elastic moduli; Micromechanics; Modeling; Mortar; Concrete

1. Introduction

It is well known that many factors including water–cement ratio, aggregate size distribution, and voids significantly affect concrete's hardened properties (see, e.g., Ref. [1]). Modeling effective properties [2] of concrete [1,Chap,12], based on constituent information, originated with approaches [3–9] that considered concrete to be a composite material composed to two constituents: aggregate and cement paste. Nilsen and Monteiro [10] (see also Ref. [11]), however, observed that elastic moduli data for concrete violated the lower Hashin–Shtrikman [12] bounds [13] and thus proposed that the presence of the interfacial transition zone (ITZ) constituted a third phase in concrete in addition to aggregate and cement paste. Subsequent models [14–17] that incorporate a homogeneous ITZ have been developed. However, as recently supported in a review [18], the gradient nature of the ITZ is important. Incorporating the gradient nature of the ITZ has been addressed [19–21]. The approach taken by Nadeau [21], which is outlined in the remainder of this section, models the local volume fraction of cement through the ITZ, which, in turn, gives rise to local water–cement ratios, then to local property variations through the ITZ, and, finally, to arrive at a model for the effective elastic properties of mortar.

For a mortar with equisized spherical aggregates, the radial distribution in the local cement volume fraction α_c has been modeled [21] by

$$\alpha_c(r) = \begin{cases} \overline{\alpha}_c\left[1 + a_c\left(\frac{r-r_a-\delta}{\delta}\right)^2\right] & r_a \le r \le r_a + \delta \\ \overline{\alpha}_c & r \ge r_a + \delta \end{cases} \quad (1)$$

based on numerical computations by Scrivener and Pratt [22], where r_a is the aggregate radius, δ is the width of the ITZ, $\overline{\alpha}_c$ is the local cement volume fraction in the non-ITZ cement paste, and a_c is a constant equal to approximately -0.5. The quantity $\overline{\alpha}_c$ is derivable in terms of the overall water–cement ratio w_o, specific gravity of cement G_c, and volume fraction of aggregate c_a by requiring the conservation of cement:

$$\overline{\alpha}_c = \frac{10(1-c_a)}{(1+w_o G_c)\left[a_c c_a \frac{\delta}{r_a}\left\{\left(\frac{\delta}{r_a}\right)^2 + 5\left(\frac{\delta}{r_a}\right) + 10\right\} + 10(1-c_a)\right]}. \quad (2)$$

* Tel.: +1-919-660-5216; fax: +1-919-660-5219.
E-mail address: nadeau@duke.edu (J.C. Nadeau).

0008-8846/03/$ – see front matter © 2003 Elsevier Science Ltd. All rights reserved.
PII: S0008-8846(02)00931-6

The local water–cement ratio w is

$$w = \frac{\alpha_w}{G_c \alpha_c} \tag{3}$$

where α_w is the local volume fraction of water and G_c is the specific gravity of the cement. By "local", it is meant constituents whose scale is much smaller than that of the fine aggregate (FA). Thus, if cement and water are the only constituents at this smaller scale then $\alpha_w = 1 - \alpha_c$.

Based on published experimental results, the bulk κ_{cp} and shear μ_{cp} moduli for saturated cement pastes were modeled [21] as a function of water–cement ratio by

$$\kappa_{cp} = \begin{cases} c_\kappa + d_\kappa w + e_\kappa w^2, & 0.2 < w \le \overline{w}_\kappa \\ a_\kappa \exp(b_E w) + \kappa_{water}, & w \ge \overline{w}_\kappa \end{cases} \tag{4}$$

$$\mu_{cp} = \begin{cases} c_\mu + d_\mu w + e_\mu w^2, & 0.2 < w \le \overline{w}_\mu \\ a_\mu \exp(b_E w) + \mu_{water}, & w \ge \overline{w}_\mu \end{cases} \tag{5}$$

where

$$d_\kappa = a_\kappa b_E \exp(b_E \overline{w}_\kappa) - 2 e_\kappa \overline{w}_\kappa \tag{6}$$

$$c_\kappa = a_\kappa \exp(b_E \overline{w}_\kappa) + \kappa_{water} - d_\kappa \overline{w}_\kappa - e_\kappa \overline{w}_\kappa^2 \tag{7}$$

$$d_\mu = a_\mu b_E \exp(b_E \overline{w}_\mu) - 2 e_\mu \overline{w}_\mu \tag{8}$$

$$c_\mu = a_\mu \exp(b_E \overline{w}_\mu) + \mu_{water} - d_\mu \overline{w}_\mu - e_\mu \overline{w}_\mu^2 \tag{9}$$

where $\kappa_{water} = 2.0$ GPa and $\mu_{water} = 0$ GPa. As described in detail in Ref. [21], the fitting parameters (b_E, a_κ, e_κ, $\overline{w}_\kappa$, a_μ, e_μ, $\overline{w}_\mu$) were determined from least squares analyses using the data in Refs. [11,23] to yield

$$b_E = -3.3754 \tag{10}$$

$$a_\kappa = 65.8999 \text{ GPa}, \quad e_\kappa = -117.3764 \text{ GPa}, \quad \overline{w}_\kappa = 0.4142 \tag{11}$$

$$a_\mu = 36.6103 \text{ GPa}, \quad e_\mu = -84.8249 \text{ GPa}, \quad \overline{w}_\mu = 0.3892 \tag{12}$$

Application of the model to data on saturated mortars resulted in a calculated ITZ thickness of 48.3 μm [21].

2. Embedded constituents with size distributions

Consider a cementitious composite consisting of $\overline{k}$ constituents (e.g., FA, coarse aggregate (CA), entrapped air (EPA)), each potentially possessing a size distribution of particles, which are embedded within the cement paste. Consider the kth constituent (where $k \in \{1, 2, 3, \ldots, \overline{k}\}$) with a volume fraction c_k and composed of n_k distinct particle sizes s_i^k where $i \in \{1, 2, 3, \ldots, n_k\}$ according to

$$s_1^k > s_2^k > s_3^k > \cdots > s_{n_k}^k. \tag{13}$$

The relative volume of particles of size s_i^k relative to the total volume of the kth constituent is denoted by f_i^k. As a result, $\sum_{i=1}^{n_k} f_i^k = 1$ for all $k \in \{1, 2, 3, \ldots, \overline{k}\}$.

As a particular example, it may be that information regarding the size distribution of particles for a constituent comes from a sieve analysis. Consider n sieves where the ith sieve has opening dimension s_i. The sieves are numbered from largest to smallest:

$$s_1 > s_2 > s_3 > \cdots > s_n. \tag{14}$$

Let w_i denote the weight of aggregate retained on the ith sieve, with opening size s_i. It follows that the relative fraction of the sample that is retained on the ith sieve is given by $f_i = w_i / (\sum_j w_j)$. It is assumed that all of the sample passes through the largest sieve; in other words, $w_1 = 0$.

Let $c_{ncp} = \sum_{k=1}^{\overline{k}} c_k$ denote the volume fraction of all constituents embedded within the cement paste ("ncp" is an acronym for noncement paste, which, in this paper, is equivalent to the union of FA, entrapped voids, and CA); the remaining fraction, $1 - c_{ncp}$, is thus cement paste. The volume of cement paste within a shell of thickness d surrounding the kth constituent per unit volume of constituent is denoted by S_d^k. It follows that the volume of ITZ paste per volume of all $\overline{k}$ constituents is given by

$$S_d = \frac{1}{c_{ncp}} \sum_{k=1}^{\overline{k}} c_k S_d^k. \tag{15}$$

The corresponding volume of cement paste within the shells of thickness d is $S_d c_{ncp}$, which must be less than $1 - c_{ncp}$, the volume of cement paste. When $d = \delta$, we denote S_d as S_δ. Therefore, if $S_\delta > c_{ncp}/(1 - c_{ncp})$, then the shells of thickness δ overlap, and it is necessary to determine $0 \le d < \delta$ such that $S_d = (1 - c_{ncp})/c_{ncp}$. Another approach [20] has been adopted for computing the ITZ volume based on Ref. [24], which utilizes statistical measures of the particle size distributions.

If $S_\delta > (1 - c_{ncp})/c_{ncp}$, then there is not enough cement paste to coat every aggregate with at least a thickness δ of paste. In this case, each aggregate is coated with a thickness of cement paste given by the solution of the equation

$$S_d - \frac{1 - c_{ncp}}{c_{ncp}} = 0 \tag{16}$$

for d, where S_d is a function of d. The thickness of the shell $\hat{\delta}$ surrounding each aggregate within which the water–cement ratios are gradient in nature is thus given by

$$\hat{\delta} = \begin{cases} \delta, & S_\delta \le c_{ncp}/(1-c_{ncp}) \\ \text{real root of Eq.(16)}, & S_\delta \ge c_{ncp}/(1-c_{ncp}). \end{cases} \quad (17)$$

Baring a more specific analysis of the aggregates to determine S_d as a function of d, S_d is readily approximated if the aggregates are assumed to be spherical. Assuming that the average radius of the particles retained on the ith sieve is r_i^k it follows that

$$S_d^k = \sum_{i=1}^{n_k} f_i^k \left[\left(1 + \frac{d}{r_i^k} \right)^3 - 1 \right]. \quad (18)$$

Substituting Eq. (18) into Eq. (15) and then that result into Eq. (16) yields

$$\sum_{k=1}^{\bar{k}} \sum_{i=1}^{n_k} \frac{c_k f_i^k}{(r_i^k)^3} d^3 + 3 \sum_{k=1}^{\bar{k}} \sum_{i=1}^{n_k} \frac{c_k f_i^k}{(r_i^k)^2} d^2 + 3 \sum_{k=1}^{\bar{k}} \sum_{i=1}^{n_k} \frac{c_k f_i^k}{r_i^k} d - (1 - c_{ncp}) = 0 \quad (19)$$

which is a third-order polynomial, the real root of which yields the effective thickness of the ITZ $\hat{\delta}$ when there is insufficient cement paste to coat all of the particles with a thickness δ.

One possible association between the average radius r_i of aggregates retained on the ith sieve with opening size s_i is

$$r_i^k = (s_i^k + s_{i-1}^k)/4, \quad (20)$$

but other associations are possible.

Because graded aggregates are utilized here, it is assumed that there is a space filling of aggregate sizes such that it is possible to achieve a situation where all of the cement paste resides within ITZ zones, yet no ITZ zones overlap. This occurs in the proposed model when $\hat{\delta} < \delta$. Assuming this size distribution exists when considering all of the $\bar{k}$ embedded constituents, the approach of Nadeau [21] may be generalized to yield the following radial variation in the local, volume fraction of cement

$$\alpha_c^i(r) = \begin{cases} \bar{\alpha}_c \left[1 + a_c \left(\frac{r - r_i - \delta}{\delta} \right)^2 \right], & r_i \le r \le r_i + \hat{\delta} \\ \bar{\alpha}_c & r \ge r_i + \hat{\delta}. \end{cases} \quad (21)$$

As will be made clearer in the following developments, if $\hat{\delta} < \delta$, then $r \ge r_i + \hat{\delta}$ will not be considered.

By requiring the conservation of relative proportion of cement, it is straightforward (following the approach of Nadeau [21]) to arrive at the following expression for $\bar{\alpha}_c$:

$$\bar{\alpha}_c = \frac{10(1 - c_{ncp})}{(1 + w_o G_c)[a_c c_{ncp} \Delta + 10(1 - c_{ncp})]}, \quad (22)$$

where

$$\Delta := \sum_{k=1}^{\bar{k}} \sum_{i=1}^{n_k} \frac{c_k f_i^k}{c_{ncp}} \left(\frac{\hat{\delta}}{r_i^k} \right) \left[\Xi_1 \left(\frac{\hat{\delta}}{r_i^k} \right)^2 + 5\Xi_2 \left(\frac{\hat{\delta}}{r_i^k} \right) + 10\Xi_3 \right] \quad (23)$$

$$\Xi_1 := 6\left(\frac{\hat{\delta}}{\delta} \right)^2 - 15\left(\frac{\hat{\delta}}{\delta} \right) + 10 \quad (24)$$

$$\Xi_2 := 3\left(\frac{\hat{\delta}}{\delta} \right)^2 - 8\left(\frac{\hat{\delta}}{\delta} \right) + 6 \quad (25)$$

$$\Xi_3 := \left(\frac{\hat{\delta}}{\delta} \right)^2 - 3\left(\frac{\hat{\delta}}{\delta} \right) + 3. \quad (26)$$

When $\hat{\delta} = \delta$, $\bar{k} = 1$, and $n_1 = 1$, the result in Ref. [21] is recovered.

3. Effective property model

In order to incorporate particle size distributions in a tractable manner each embedded constituent is modeled as a spherical inclusion with a radius determined such that the volume fraction of ITZ (with thickness $\hat{\delta}$) associated with a constituent and the volume fraction of the constituent itself is conserved. This radius for the kth embedded constituent is denoted by $\tilde{r}_k$ and will be termed an equivalent radius. It is readily shown that the equivalent radius given by

$$\tilde{r}_k = \frac{\hat{\delta}}{\sqrt[3]{1 + S_{\hat{\delta}}^k} - 1} \quad (27)$$

will conserve the relative proportion of ITZ volume associated with a constituent to the volume of that constituent. Note that S_δ^k is Eq. (18) evaluated with $d = \hat{\delta}$.

We consider, in general, $\bar{k}$ embedded constituents. For clarity, however, in the remainder of this section and the results presented in the following section, only three embedded constituents are considered (i.e., $\bar{k} = 3$): FA, entrapped voids that may be partially or completely filled with water, and CA. As such, it will be convenient to refer to these constituents as FA, EPA, and CA rather than 1, 2, and 3, respectively. Typical ranges in particle sizes for each of

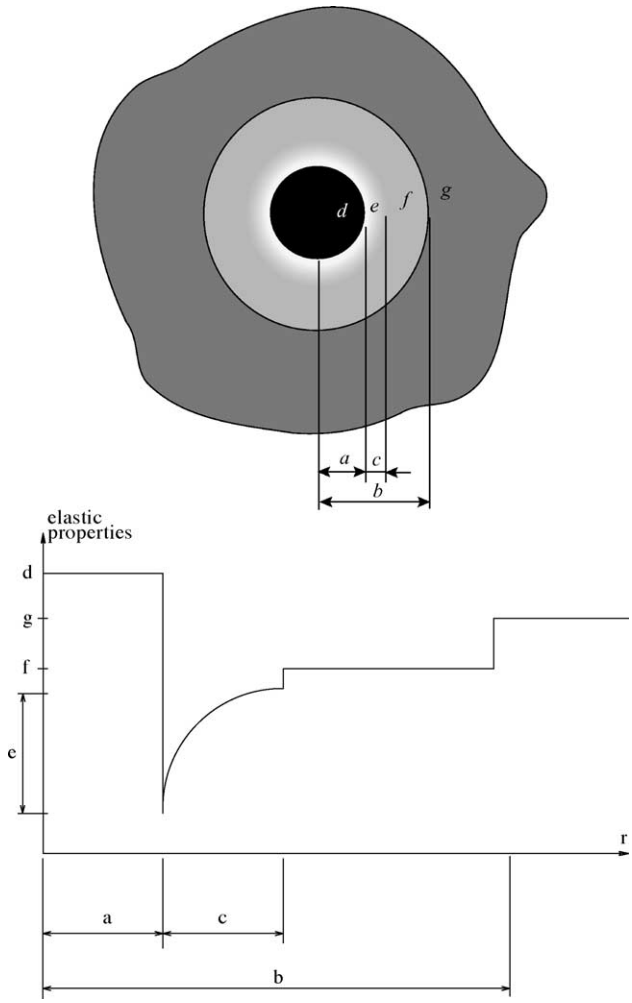

Fig. 1. Depiction of generalized self-consistent model at a given scale (i.e., FA, EPA, or CA). The top portion illustrates a cross-sectional view through a typical inclusion and the bottom portion illustrates the radial variation in the elastic properties. The letters a–c represent distances, and the letters d–g represent material properties. More specifically, a denotes the radius of the inclusion particle, b is radius of the concentric sphere, which is determined to maintain the relative proportions of all constituents, and c is the thickness of the region within the cement paste with gradient material properties. d are the elastic properties of the inclusion, e are the elastic properties through the ITZ, f are the effective elastic properties from the previous (smaller) scale, and g are the effective material properties at the scale under consideration. At a given scale, quantities a–f are inputs to the model and g is the quantity to be computed.

these three classifications of embedded constituents are 0.075–4.75, 1–3, and 4.75–40 mm.

A succession of homogenizations are to be implemented below, one at each scale comparable to the equivalent radii, provided that the equivalent radii of the embedded constituents are well separated

$$\tilde{r}_{\mathrm{FA}} \ll \tilde{r}_{\mathrm{EPA}} \ll \tilde{r}_{\mathrm{CA}}. \tag{28}$$

More specifically, this may mean, for example, at least an order of magnitude difference between any two equivalent radii. The type of homogenization employed is a generalized self-consistent method. The description of the model presented below proceeds from the largest scale (CA) to the smallest scale (FA) when, in fact, the actual computations need to be performed from the smallest scale to the largest.

Given the well-separated length scales, the model develops by assuming that the equivalent CA particle, with its ITZ of thickness $\hat{\delta}$, is embedded within a sphere whose properties are the effective properties at the length scale of the EPA, κ^*_{EPA} and μ^*_{EPA}. The radius of this sphere, which we will denote as b, will be discussed separately below. The "composite sphere" (this is a generalization of the term used by Hashin [25] to include the ITZ) of radius b is embedded within an infinite matrix whose properties are the effective properties at the length scale of the CA, κ^*_{CA} and μ^*_{CA}, which are, in fact, the effective properties of the concrete, $\kappa^* \equiv \kappa^*_{\mathrm{CA}}$ and $\mu^* \equiv \mu^*_{\mathrm{CA}}$. A general depiction of this model is given in Fig. 1 in terms of quantities a–g. The general definition and specific interpretation of each of these quantities is detailed in the caption to Fig. 1 and the "CA" column of Table 1, respectively.

Similarly, the effective properties at the length scale of the EPA, κ^*_{EPA} and μ^*_{EPA}, are modeled by considering the equivalent EPA particle, with its ITZ of thickness $\hat{\delta}$, embedded within a sphere whose properties are the effective properties at the length scale of the FA, κ^*_{FA} and μ^*_{FA}. This "composite sphere" is embedded within an infinite matrix whose properties are the effective properties at the length scale of the EPA. Refer to Fig. 1 and the "EPA" column of Table 1.

Finally, the effective properties at the length scale of the FA, κ^*_{FA} and μ^*_{FA}, are modeled by considering the equivalent FA particle, with its ITZ of thickness $\hat{\delta}$, embedded within a sphere whose properties are those of the cement paste. This "composite sphere" is embedded within an infinite matrix whose properties are the effective properties at the length scale of the FA. Refer to Fig. 1 and the "FA" column of Table 1.

In reference to Fig. 1, the radius b of the "composite sphere" is determined such that the volume fraction of the particle with radius $\tilde{r}$ is maintained. Because, at a given

Table 1
Specific interpretation of the general quantities a–g presented in Fig. 1 for homogenization at length scales representative of each of the three embedded constituents considered: FA, EPA, and CA

	Homogenization at scale of …		
	FA	EPA	CA
a	$\tilde{r}_{\mathrm{FA}}$	$\tilde{r}_{\mathrm{EPA}}$	$\tilde{r}_{\mathrm{CA}}$
b	$\tilde{r}_{\mathrm{FA}}/\sqrt[3]{\tilde{c}_{\mathrm{FA}}}$	$\tilde{r}_{\mathrm{EPA}}/\sqrt[3]{\tilde{c}_{\mathrm{EPA}}}$	$\tilde{r}_{\mathrm{CA}}/\sqrt[3]{\tilde{c}_{\mathrm{CA}}}$
c	$\hat{\delta}$	$\hat{\delta}$	$\hat{\delta}$
d	κ_{FA}, μ_{FA}	κ_{EPA}, μ_{EPA}	κ_{CA}, μ_{CA}
e	κ_{cp}, μ_{cp}	κ_{cp}, μ_{cp}	κ_{cp}, μ_{cp}
f	κ_{cp}, μ_{cp} at $r=\tilde{r}_{\mathrm{FA}}+\hat{\delta}$	κ^*_{FA}, μ^*_{FA}	κ^*_{EPA}, μ^*_{EPA}
g	κ^*_{FA}, μ^*_{FA}	κ^*_{EPA}, μ^*_{EPA}	$\kappa^*_{\mathrm{CA}}\equiv\kappa^*$, $\mu^*_{\mathrm{CA}}\equiv\mu^*$

Table 2
Elastic properties for FA and CA [28]

Elastic property	Value
Bulk modulus, κ	44 GPa
Shear modulus, μ	37 GPa
Young's modulus, E	88.7 GPa
Poisson's ratio, ν	0.172

scale, larger length scales are not perceived the apparent volume fraction is larger than the volume fraction apparent at a larger length scale. Furthermore, because the ITZ is modeled at each length scale, it must be observed that the ITZ associated with features at a larger length scale is also not perceived at the given length scale. For example, when homogenizing at the length scale of the FA the only recognizable constituents are the FA and the cement paste not associated with ITZs of the EPA and CA. Because of this, the apparent FA volume fraction $\tilde{c}_{FA}$ at the length scale of the FA is volume fraction of the FA, c_{FA}, divided by the volume fraction of cement paste not associated with the ITZs of the EPA and CA which is given by $1-c_{EPA}(1+(\hat{\delta}/\tilde{r}_{EPA}))^3-c_{CA}(1+(\hat{\delta}/\tilde{r}_{CA}))^3$. From this apparent volume fraction $\tilde{c}_{FA}$, the radius b for the model at the scale of the FA can be computed

$$b_{FA}=\frac{\tilde{r}_{FA}}{\sqrt[3]{\tilde{c}_{FA}}}. \tag{29}$$

Summarizing the apparent volume fraction at the scale of the FA and reporting the apparent volume fraction at the scale of the EPA and CA yields

$$\tilde{c}_{FA}=\frac{c_{FA}}{1-c_{EPA}\left(1+\frac{\hat{\delta}}{\tilde{r}_{EPA}}\right)^3-c_{CA}\left(1+\frac{\hat{\delta}}{\tilde{r}_{CA}}\right)^3} \tag{30}$$

$$\tilde{c}_{EPA}=\frac{c_{EPA}}{1-c_{CA}\left(1+\frac{\hat{\delta}}{\tilde{r}_{CA}}\right)^3} \tag{31}$$

$$\tilde{c}_{CA}=c_{CA}. \tag{32}$$

More generally, the apparent volume fraction $\tilde{c}_k$ for the kth constituent is given by

$$\tilde{c}_k=\frac{c_k}{1-\sum_{i=k+1}^{\overline{k}} c_i\left(1+\frac{\hat{\delta}}{\tilde{r}_i}\right)^3} \tag{33}$$

The b radii are given by $\tilde{r}/\sqrt[3]{\tilde{c}}$.

With respect to the specific calculation of effective properties, one must proceed from the smallest length scale to the largest length scale. At any given length scale (FA, EPA, or CA), the effective properties are computed using the generalized self-consistent n-layer sphere model [26]. The variable elastic properties through the ITZ (e.g., $\tilde{r}_{FA}\le r\le\tilde{r}_{FA}+\hat{\delta}$) are discretized as a piecewise uniform variation in properties. In particular, for the computations presented here, the ITZ was divided into 50 equal divisions along the radial direction.

The effective Young's modulus E^* and Poisson's ratio ν^* of the concrete can be computed from the familiar relations:

$$E=\frac{9\kappa\mu}{3\kappa+\mu}\qquad \nu=\frac{3\kappa-2\mu}{2(3\kappa+\mu)}. \tag{34}$$

The results presented in Section 4 will be in terms of Young's modulus E and Poisson's ratio ν. Experimental results [27] indicate that the tensile and compressive Young's moduli for concrete are effectively equal over all aggregate volume fractions.

4. Results

The previous sections have developed a model for the effective elastic properties of concrete. The model is a function of the volume fractions, size distributions, and elastic properties of FA and CA and entrapped voids. Furthermore, the model is a function of the overall water–cement ratio and specific gravity of cement. The volume fractions of the FAs and CAs and the entrapped voids, together with the overall water–cement ratio, define the volume fractions of cement and water. These total fractions are maintained, but how they are distributed on a local level through the ITZ is a function of the parameter a_c and the thickness of the ITZ δ. Based on previous analyses [21] with experimental data, $a_c=-0.5$ and $\delta=50$ μm are utilized exclusively herein.

To investigate the effect of the dependencies of the model on its predictions of effective moduli, we consider below two classes of aggregate samples: typical, sieved FA and CA samples, and an ideal, densely graded aggregate where the distinction between fine and coarse is made

Table 3
Representative CA and FA grading distributions. Equivalent radius columns present the average radius of particles retained on the given sieve as per Eq. (20)

CA			FA		
Sieve size	Equivalent radius [μm]	% Retained	Sieve size	Equivalent radius [μm]	% Retained
1 1/2 in.	n/a	0.0	No. 4	n/a	0.0
1 in.	15625	1.3	No. 8	1778	9.3
3/4 in.	11000	23.2	No. 16	885	30.1
3/8 in.	7125	67.6	No. 30	445	24.6
No. 4	3563	7.6	No. 50	225	18.7
Pan	1188	0.3	No. 100	113	10.7
			No. 200	56.3	6.4
			Pan	18.8	0.2

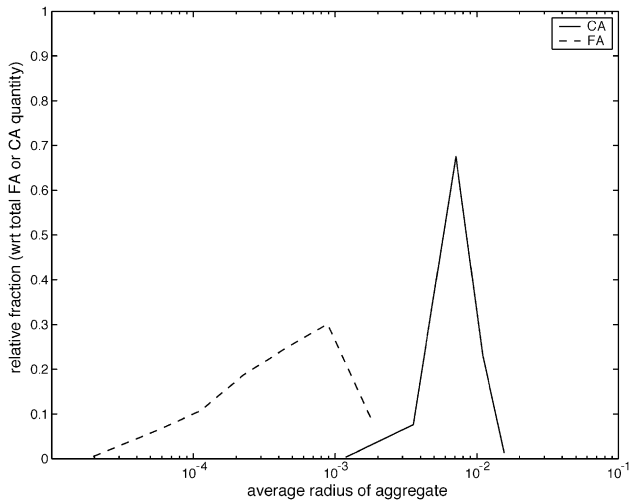

Fig. 2. Size distributions of representative CA and FA samples. Note that the total area under each curve is 1.0.

based on an aggregate size of 4.75 mm. The motivation for considering a densely graded aggregate sample is for ease of investigating the effect of the maximum aggregate size on the effective elastic properties. In both classes of aggregates, for both FA and CA, the elastic properties [28] are presented in Table 2.

The entrapped voids are taken to be of 2.0 mm uniform diameter and partially filled with water, thus, $\kappa_{EPA}=0.0$ GPa and $\mu_{EPA}=0.0$ GPa.

4.1. Typical, sieved aggregate samples

Table 3 presents sieve analyses for typical CA and FA samples. The equivalent radii of the FA and CA samples, for $\delta=\delta=50$ μm, are 193 and 7088 μm, respectively. The size gradations of both the FAs and CAs are illustrated in Fig. 2.

Fig. 3 presents the effect of the overall water–cement ratio w_o on the effective Young's modulus and Poisson's ratio (solid line) for a concrete with 25 vol.% FA, 50 vol.% CA, and 4 vol.% entrapped voids. It is observed that as the water–cement ratio ranges from 0.2 to 0.8, the Young's modulus decreases more than 50% while the Poisson ratio increases nearly 20%. To ascertain the effect of the ITZ, the effective moduli predicted without an ITZ is also presented (dashed line). It is observed that the effect of accounting for the ITZ decreases the effective Young's modulus.

An investigation into the effect of aggregate, in regards to quantity and relative proportions of fine and coarse, on the effective elastic properties was conducted and the results are presented in Figs. 4, 5, and 6 for an overall water–cement ratio of $w_o=0.45$. Fig. 4 presents the effect of

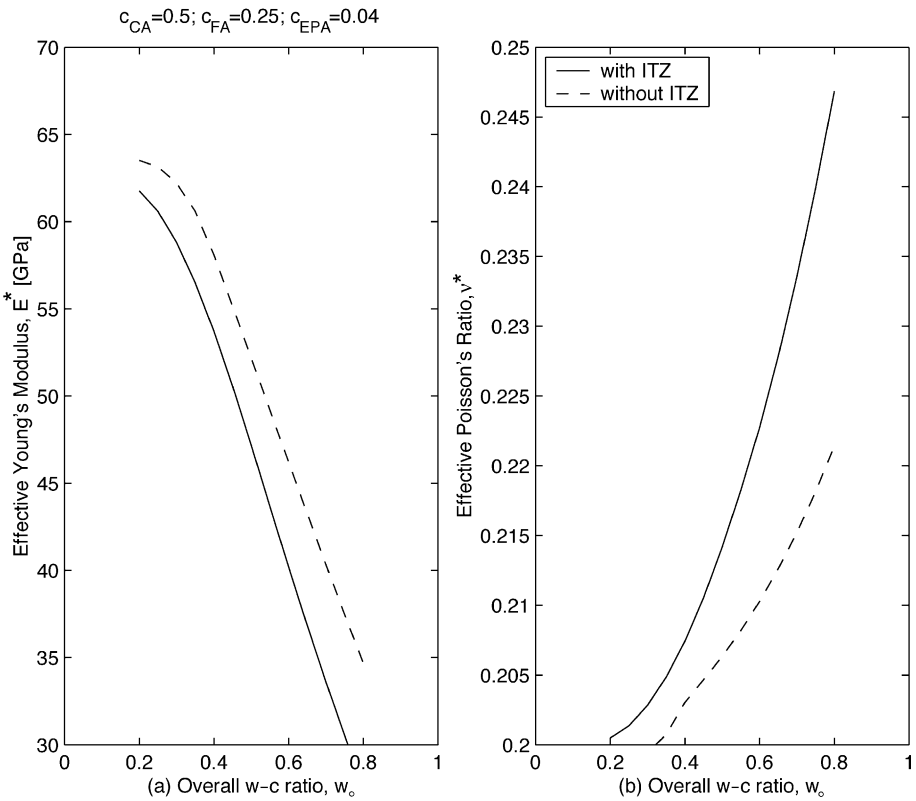

Fig. 3. Effect of overall water–cement ratio w_o on (a) Young's modulus E and (b) Poisson's ratio ν where the solid line denotes predictions of the model with a 50-μm ITZ, and the dashed line denotes results for no ITZ. The volume fractions of CA and FA are $c_{CA}=0.5$ and $c_{FA}=0.25$, respectively, and there is a $c_{EPA}=0.04$ volume fraction of entrapped air.

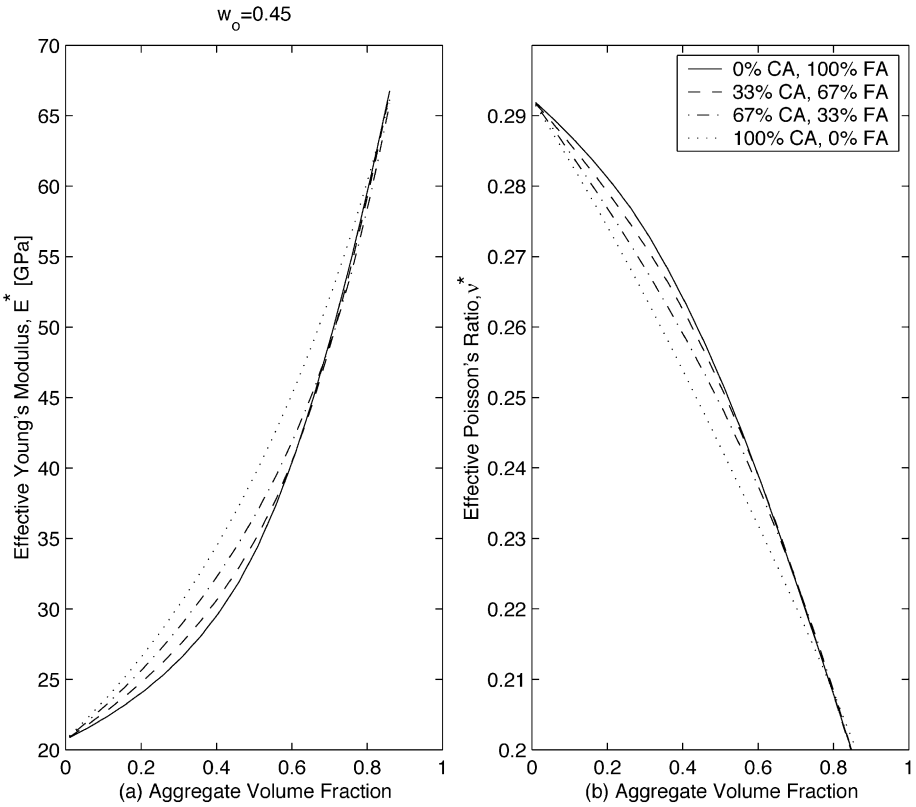

Fig. 4. Effect of total volume of aggregate on (a) Young's modulus E and (b) Poisson's ratio ν for various relative proportions of CA and FA. The overall w−c ratio is $w_o = 0.45$.

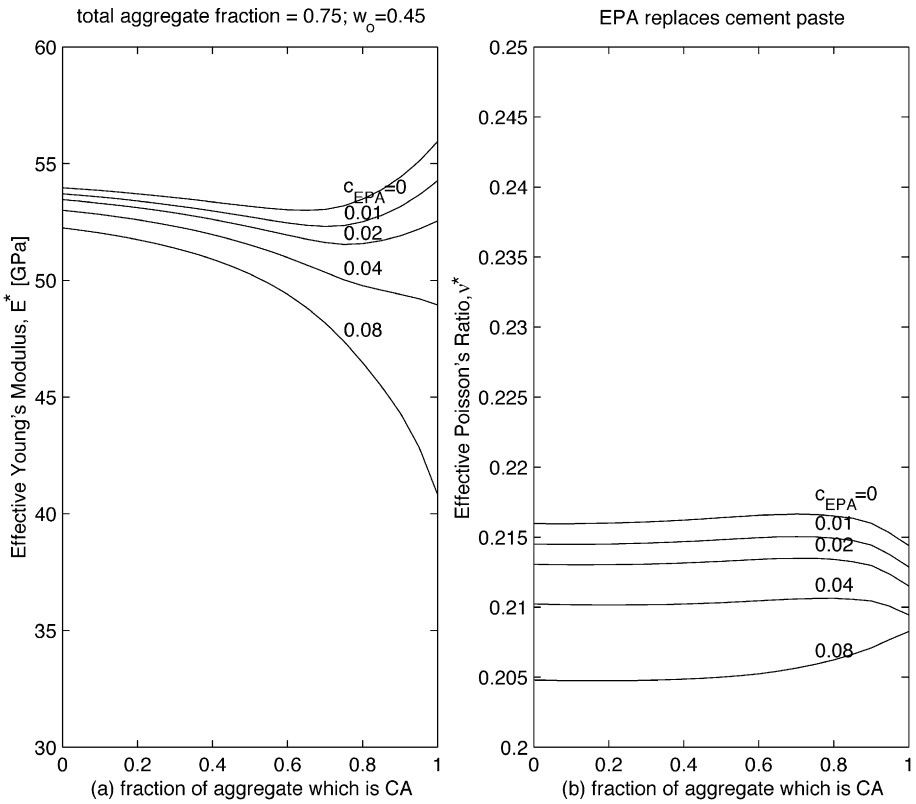

Fig. 5. Effect of relative proportions of coarse and fine aggregates on (a) Young's modulus E and (b) Poisson's ratio ν for various fractions of entrapped air, c_{EPA}; the entrapped air replaces cement paste. The overall w−c ratio is $w_o = 0.45$ and the total fraction of aggregate is 0.75.

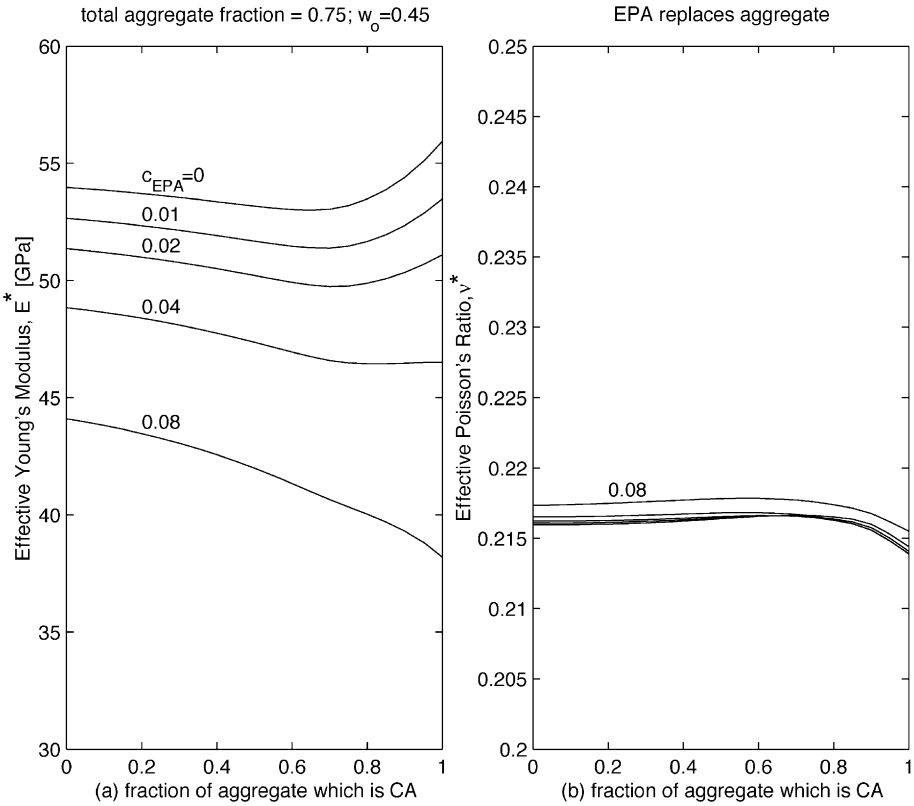

Fig. 6. Effect of relative proportions of coarse and fine aggregates on (a) Young's modulus E and (b) Poisson's ratio ν for various fractions of entrapped air, c_{EPA}; the entrapped air replaces aggregate. The overall w–c ratio is $w_o = 0.45$ and the total fraction of aggregate, without any entrapped air, is 0.75.

volume of aggregate for various relative proportions of coarse to FA with an entrapped void fraction of $c_{EPA} = 0$. The total quantity of aggregate quite significantly effects the elastic properties of the relative proportions of CA and FA is much less pronounced. In fact, for typical aggregate fractions in the range of 0.6–0.8 (with $c_{EPA} = 0$), the effective properties are nearly independent of the relative proportions of CA and FA.

Figs. 5 and 6 elaborate on the effect of relative proportions of CA and FA for various fractions of entrapped voids. The difference between the two figures is that as the entrapped void fraction increases, in Fig. 5, cement paste is displaced and the total aggregate fraction remains constant at 0.75, while in Fig. 6, aggregate content is displaced and the total cement paste fraction remains constant at 0.25. It is generally observed that the relative proportions of CAs and FAs more dramatically affect the concrete's Young's modulus as the entrapped void fraction increases while the Poisson ratio remains relatively unaffected. More specifically, for a fixed total aggregate content of 0.75 (see Fig. 5), Young's modulus is much more significantly effected by entrapped voids at larger fractions of CA than fine. For a constant 0.25 fraction of cement paste, the effect of relative proportions of CA and FA is less pronounced but more uniformly affected by increasing void content.

Fig. 7 presents the effect of entrapped void content on the elastic properties of concrete with a water–cement ratio of $w_o = 0.45$. When there is no entrapped voids, the fractions of CA and FA are $c_{CA} = 0.5$ and $c_{FA} = 0.25$, and, thus, a cement paste fraction of 0.25. The three curves presented in the figure depict the effect on the elastic properties as the increasing fraction of entrapped voids replaces cement paste (solid line), FA (dotted line), and CA (dashed line). The upper- and lowermost curves give an indication of the possible range in which the elastic properties may vary with the addition of entrapped voids.

4.2. Densely graded aggregate

To investigate the effect of maximum aggregate size on the elastic properties, as well as the effect of different aggregate gradations, we consider a densely graded aggregate sample. Aggregate grading is given by [16]

$$D(r) = \left(\frac{r - r_{\min}}{r_{\max} - r_{\min}}\right)^m \tag{35}$$

where $D(r)$ denotes the fraction of aggregate with a radius smaller than r. Plots of this gradation for $m = 0.4$

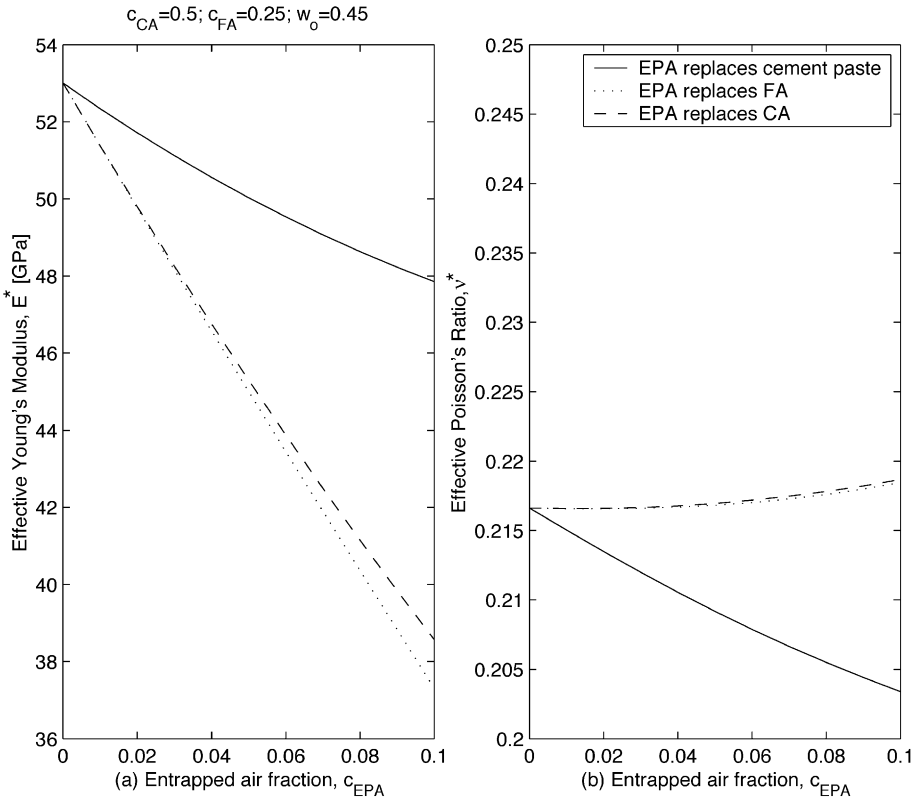

Fig. 7. Effect of entrapped air content c_{EPA} on (a) Young's modulus E and (b) Poisson's ratio ν. The three types of curves, solid, dashed, and dotted, correspond to the EPA replacing cement paste, CA, and FA, respectively. The overall w–c ratio is $w_o = 0.45$, and the fractions of CA and FA, prior to the addition of EPA, is 0.5 and 0.25, respectively.

and $m = 0.5$, which are utilized herein and correspond to a relatively "finer" and "coarser" aggregate, respectively, are presented in Fig. 8. A particle diameter of 4.75 mm is used as a cutoff to distinguish between CA and FA.

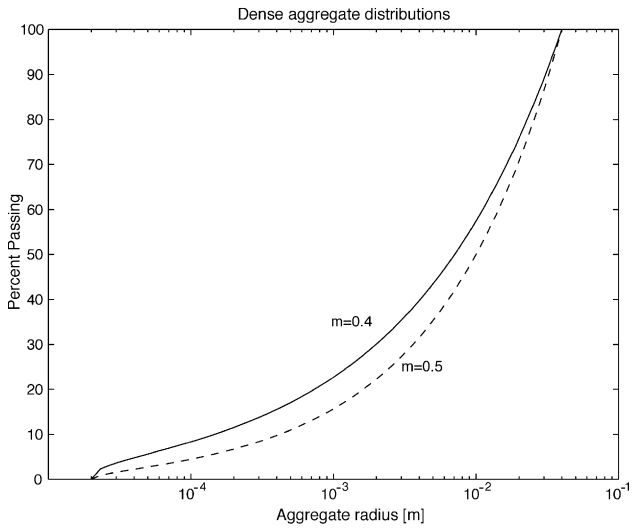

Fig. 8. Grading curves for two densely graded aggregates. The grading curve for $m = 0.4$ corresponds to a finer aggregate sample relative to the $m = 0.5$ curve.

Fig. 9 presents the effect of maximum aggregate size on the elastic properties of concrete for several overall water–cement ratios ($w_o = 0.35$, 0.45, and 0.55) for the two aggregate gradations ($m = 0.4$, solid line; $m = 0.5$, dashed line) presented in Fig. 8. Common to all these results are a total aggregate fraction of 0.75 and an entrapped void fraction of $c_{EPA} = 0.04$. General trends indicate that the Young's modulus increases with (a) decreasing maximum aggregate size, and (b) increasing "coarseness" of the aggregate. The effect on Poisson's ratio is minor.

The finding observed above that the effective Young's modulus E^* increases with decreasing maximum aggregate size is in difference to another analytical finding [16], which supports its finding with published experimental results [29]. It is not clear, however, that these experimental results [29] are qualitatively in keeping with the prediction of the authors of [16], because the experimental samples, which had different maximum aggregate sizes, also had different volume fractions of aggregate. From Fig. 4, it was observed that the volume fraction of aggregate has a very significant effect on the effective Young's modulus of concrete, and this factor is also at play in contributing to the qualitative

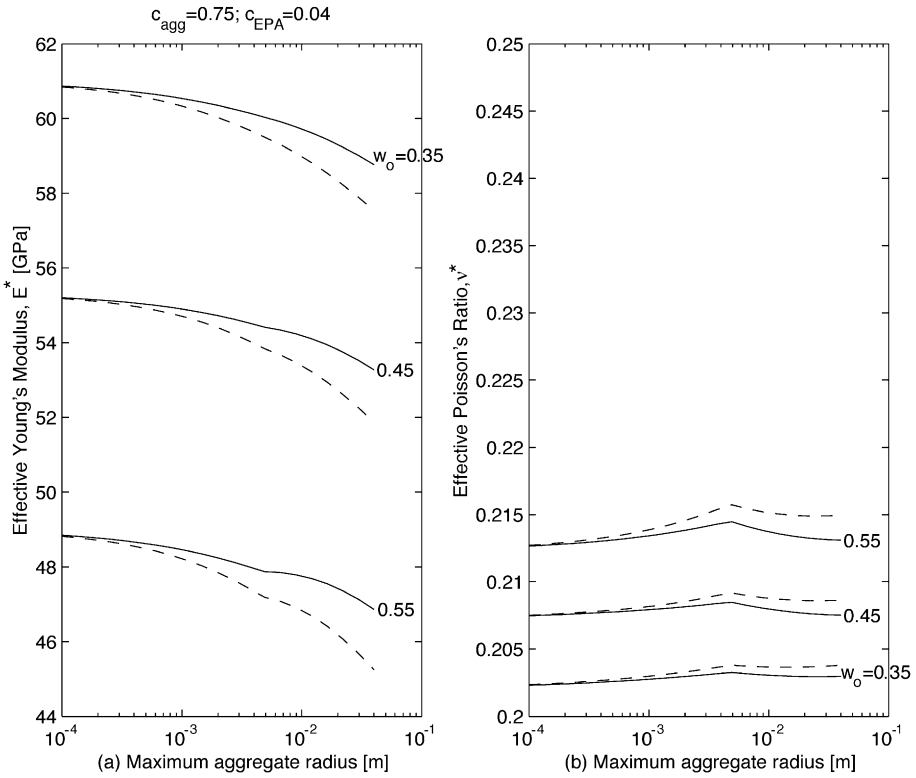

Fig. 9. Effect of maximum aggregate size and overall w–c ratio on (a) Young's modulus E and (b) Poisson's ratio ν for the two aggregate samples depicted in Fig. 8; the solid line is for $m=0.4$ and the dashed line is for $m=0.5$. The total aggregate fraction is 0.75 and the entrapped air content is $c_{\mathrm{EPA}}=0.04$.

nature of the results, in addition to the maximum size of aggregate.

5. Discussion and closure

This paper has presented a multiscale model for the effective elastic properties of concrete that incorporates water–cement ratio gradients through the ITZ, FA and CA size distributions, and entrapped voids. The model is valid at large volume fractions. Most significantly, the model conserves the total volumes of cement and water, or their relative proportions to maintain a specified overall water–cement ratio. This conservation cannot be assured in approaches that require either directly or indirectly the specification of elastic properties for all constituents.

Unfortunately, the author neither currently possesses nor is aware of sufficient experimental data that could be used to validate this model. However, a previous study [21] utilized a special case of the model presented herein to calculate the ITZ thickness to be 48.3 μm. This calculation is consistent with visual inspection of the ITZ thickness from SEM micrographs.

The model as presented above exclusively treats entrapped voids in distinction from entrained voids. The size of entrained voids, which are typically on the order of 50–200 μm, are moderately larger than the length scale of cement particles. It was beyond the scope of the present paper to incorporate this constituent, but this is a topic of future research.

If an empirical relation between concrete's Young's modulus E^* and compressive strength f_c' is admitted, it is possible to extrapolate the results of this paper toward the compressive strength of concrete. One such relation [30] is

$$E^* = 0.043(\rho^*)^{1.5}\sqrt{f_c'} \tag{36}$$

where ρ^* is the density of concrete, in units of kg/m^3, and f_c' is the compressive strength of concrete, in units of MPa. The units of E^* are also MPa and ρ^* is restricted to be within 1410 and 2430 kg/m^3. Solving Eq. (36) for the compressive strength of the concrete yields

$$f_c' = 541\left(\frac{E^*}{(\rho^*)^{1.5}}\right)^2, \tag{37}$$

which, in turn, yields an empirical trend that the compressive strength increases with increasing Young's modulus and decreasing density. The density of concrete, in terms of quantities utilized in the model presented in this paper, is

$$\rho^* = [1 + c_{\mathrm{FA}}(G_{\mathrm{FA}} - 1) + c_{\mathrm{EPA}}(G_{\mathrm{EPA}} - 1) + c_{\mathrm{CA}}(G_{\mathrm{CA}} - 1) + \frac{1 - c_{\mathrm{FA}} - c_{\mathrm{EPA}} - c_{\mathrm{CA}}}{1 + w_o G_c}(G_c - 1)]\rho_w, \tag{38}$$

which, together with Eq. (37), affords a means by which to design concrete mixes for strength. Obviously, employing such an empirical relation should be done with caution [31].

The results in Section 4 generally support the common observation that Poisson's ratio for typical concretes is relatively invariant [32].

References

[1] P.K. Mehta, P.J.M. Monteiro, Concrete: Microstructure, Properties, and Materials, McGraw-Hill, New York, 1993.

[2] Z. Hashin, Analysis of composite materials—a survey, J. Appl. Mech. 50 (1983) 481–505.

[3] T.C. Hansen, Creep of concrete—a discussion of some fundamental problems, Bull. Swed. Cem. Concr. Res. Inst. 33 (1958).

[4] P. Dantu, Étude des contraintes dans les milieux hétérogènes. Application au béton, Ann. Inst. Tech. Bâtim. Trav. Publics 40 (121) (1958) 54–77.

[5] M.F. Kaplan, Ultrasonic pulse velocity, dynamic modulus of elasticity, poisson's ratio and the strength of concrete made from thirteen different coarse aggregates, RILEM Bull. 1 (1959) 58–73.

[6] T.C. Hansen, Bull. Swed. Cem. Concr. Res. Inst. 37 (1960).

[7] T.J. Hirsch, Modulus of elasticity of concrete affected by elastic moduli of cement paste matrix and aggregate, J. Am. Concr. Inst. 59 (1962) 427–451.

[8] T.C. Hansen, Influence of aggregate and voids on modulus of elasticity of concrete, cement mortar, and cement paste, J. Am. Concr. Inst. 62 (2) (1965) 193–216.

[9] U.J. Counto, The effect of elastic modulus of the aggregate on the elastic modulus, creep and creep recovery of concrete, Mag. Concr. Res. 16 (48) (1964) 129.

[10] A.U. Nilsen, P.J.M. Monteiro, Concrete: a three phase material, Cem. Concr. Res. 23 (1) (1993) 147–151.

[11] P. Simeonov, S. Ahmad, Effect of transition zone on the elastic behavior of cement-based composites, Cem. Concr. Res. 25 (1) (1995) 165–176.

[12] Z. Hashin, S. Shtrikman, On some variational principles in anisotropic and nonhomogeneous elasticity, J. Mech. Phys. Solids 10 (1962) 335–342.

[13] J.C. Nadeau, M. Ferrari, On optimal zeroth-order bounds with application to Hashin–Shtrikman bounds and anisotropy parameters, Int. J. Solids Struct. 38 (2001) 7945–7965.

[14] G. Ramesh, E.D. Sotelino, W.F. Chen, Effect of transition zone on elastic moduli of concrete materials, Cem. Concr. Res. 26 (4) (1996) 611–622.

[15] C.C. Yang, Effect of the transition zone on the elastic moduli of mortar, Cem. Concr. Res. 28 (5) (1998) 727–736.

[16] G. Li, Y. Zhao, S.-S. Pang, Y. Li, Effective Young's modulus estimation of concrete, Cem. Concr. Res. 29 (1999) 1455–1462.

[17] G. Li, Y. Zhao, S.-S. Pang, Four-phase sphere modeling of effective bulk modulus of concrete, Cem. Concr. Res. 29 (1999) 839–845.

[18] A. Bentur, M.G. Alexander, A review of the work of the RILEM TC 159-ETC: Engineering of the interfacial transition zone in cementitious composites, Mater. Struct. 33 (2000) 82–87.

[19] M.P. Lutz, P.J.M. Monteiro, R.W. Zimmerman, Inhomogeneous interfacial transition zone model for the bulk modulus of mortar, Cem. Concr. Res. 27 (7) (1997) 1113–1122.

[20] E. Garboczi, D. Bentz, Analytical formulas for interfacial transition zone properties, Adv. Cem. Based Mater. 6 (1997) 99–108.

[21] J.C. Nadeau, Water-to-cement ratio gradients in mortars with application to effective elastic properties, Cem. Concr. Res. 32 (2002) 481–490.

[22] K. Scrivener, P. Pratt, Characterization of interfacial microstructure, RILEM Report, vol. 11, E&FN Spon, London, 1996, pp. 1–17 (Chap. 1).

[23] J. Wang, J. Lubliner, P. Monteiro, Effect of ice formation on the elastic moduli of cement paste and mortar, Cem. Concr. Res. 18 (1988) 874–885.

[24] B. Lu, S. Torquato, Near-surface distribution functions for polydispersed systems, Phys. Rev. A 45 (8) (1992) 5530–5544.

[25] Z. Hashin, The elastic moduli of heterogeneous materials, J. Appl. Mech. 29 (1) (1962) 143–150.

[26] E. Herve, A. Zaoui, *n*-Layered inclusion-based micromechanical modelling, Int. J. Eng. Sci. 31 (1) (1993) 1–10.

[27] A.F. Stock, D.J. Hannant, R.I.T. Williams, The effect of aggregate concentration upon the strength and modulus of elasticity of concrete, Mag. Concr. Res. 31 (109) (1979) 225–234.

[28] G.T. Kuster, M.N. Toksöz, Velocity and attenuation of seismic waves in two-phase media: Part I. Theoretical formulations, Geophysics 39 (5) (1974) 587–606.

[29] J. Vilardell, A. Aguado, L. Agullo, R. Gettu, Estimation of the modulus of elasticity for dam concrete, Cem. Concr. Res. 28 (1) (1998) 93–101.

[30] American Concrete Institute, Building Code Requirements for Structural Concrete and Commentary, American Concrete Institute, Farmington Hills, MI, 1999.

[31] O. Ishai, Discussion of Young's modulus and Poisson's ratio of concrete cured at various humidities, Mag. Concr. Res. 15 (1963) 235.

[32] M. Anson, K. Newman, The effect of mix proportions and method of testing on Poisson's ratio for mortars and concretes, Mag. Concr. Res. 18 (56) (1966) 115–130.